

# Trading Studies of a Very Large Hadron Collider \*

Alessandro G. Ruggiero

*Brookhaven National Laboratory  
Upton, New York*

## Introduction

We have shown that the design of the ELOISATRON can be approached in five separate steps [1]. In this report we shall deal with the two major issues of the collider: the size and the strength of the superconducting magnets. The reference design of the SSC calls for a collider circumference of 86 km. It represents the largest size that until recently was judged feasible. The reference design of the LHC requires a bending field of 9 Tesla, that industries are presently determined to demonstrate. Clearly the large size of the project presents problem with magnet tolerances, and collider operation and management. The high field of the superconducting magnets needs to be demonstrated, and the high-field option in excess of 9 Tesla requires extensive research and development. It is obvious from the start that, if the ELOISATRON has to allow large beam energies, the circumference has also to be larger than that of the SSC, probably of few hundred kilometers. On the other end, Tevatron, RHIC and SSC type of superconducting magnets have been built and demonstrated on a large scale and proven to be cost effective and reliable. Their field, nevertheless, hardly can exceed a value of 7.5 Tesla, without major modifications that need to be studied. The LHC type of magnets may be capable of 9 Tesla, but they are being investigated presently by the European industries. It is desired that if one wants to keep the size of the ring under reasonable limits, a somewhat higher bending field is required for the ELOISATRON, especially if one wants also to take advantage of the synchrotron radiation effects. A field value of 13 Tesla, twice the value of the SSC superconducting magnets, has recently been proposed, but it clearly needs a robust program of research and development. This magnet will not probably be of the RHIC/SSC type and not even of the LHC type. It will have to be designed and conceived anew.

In the following we shall examine two possible approaches. In the first approach, we shall take as a starting reference the SSC design with a constant circumference of 87 km. We shall investigate the energy range of 20 to 100 TeV, and include the synchrotron radiation effects. The required bending field will be calculated accordingly. In the second approach we shall follow the same as outlined in the first one, except that we shall assume a constant bending field of 13 Tesla. The circumference of the collider will then be determined accordingly. This study will show the consequences of these assumptions and approaches. In our opinion, the feasibility of the ELOISATRON need control of the overall size at one end, and a bending field which is larger than what has been demonstrated recently.

The analysis that follows makes use of more or less standard relationships which have been summarized apart [2].

\*Work performed under the auspices of the U.S. Department of Energy

## The SSC Project

As a starting point, to make a useful comparison, we list in Table 1 the major parameters of the SSC, the USA project that, after having reached an estimated cost close to 10 B\$, was official discontinued during fall of 1993. The injector of the SSC was made of a Linac and three accelerators injecting into each other: the Low, Medium, and High Energy Boosters.

Table 1: Main Parameters of the SSC

	Linac	LEB	MEB	HEB	Collider
Energy	0.6 GeV	11.1 GeV	200 GeV	2 TeV	20 TeV
Circumference, $2\pi R$ , km	--	0.54	3.96	10.89	87.12
Cycle Time	--	0.1 s	4.5 s	4.5 min	--
Number of Protons	--	$1 \times 10^{12}$	$7 \times 10^{12}$	$2 \times 10^{13}$	$1.3 \times 10^{14}$
Luminosity, $\text{cm}^{-2} \text{s}^{-1}$	--	--	--	--	$1 \times 10^{33}$
Bending Field, B, Tesla	--	--	--	--	6.55
Bending Radius, $\rho$ , km	--	--	--	--	10.2
Packing Factor, $\rho/R$	--	--	--	--	0.734
FODO Cell Length, m	--	--	--	--	180
Phase Advance / Cell	--	--	--	--	$90^\circ$
Magnet Coil i.d., mm	--	--	--	--	50
Normal. rms Emittance	--	--	--	--	$1 \pi \text{ mm mrad}$
$\beta^*$ , m	--	--	--	--	0.5
rf Frequency, MHz	--	--	--	--	360
Beam-Beam Tune-Shift	--	--	--	--	0.0005
Z/n limit, ohm	--	--	--	--	5

## Fixed-Size Approach

To study the energy dependence of the collider in the 20-100 TeV range with the fixed-size approach, we shall make use of some parameters which are common to all energies and that are closely derived from the SSC design. The parameters are listed in Table 2. We shall assume the same packing factor, and thus the same bending radius as in the SSC. The length of the FODO cells and their phase advance is also as in the SSC. The entire circumference of the collider is assumed as a continuous sequence of FODO cells. Betatron tunes and the other lattice functions and parameters are then estimated neglecting the presence and the details of special insertions. We

shall also assume the same rms normalized emittance at the end of the acceleration cycle and just at the beginning of the storage period. An important parameter which determines the aperture of the superconducting magnets is the ratio of the coil inner radius to the rms beam size when this is the largest, that is at the beginning of the storage period. This ratio is taken to be 60 and is broken down in two factors. A factor of 10 is required as the ratio between dynamic aperture and rms beam size. Another factor of 6 is the expected ratio (as estimated during the SSC design studies) between coil internal radius and dynamical aperture.

Table 2: Parameters of the Fixed-Size Approach

Circumference	87.2 km
Packing Factor	0.734
Bending Radius	10.2 km
FODO Cell Length	180 m
Phase Advance / Cell	90°
Equivalent No. of FODO Cells	484
Betatron Tune (H = V)	121
Bending Angle / Cell	13.0 mrad
$\beta$ - max	307
$\eta$ - max	1.58
$\gamma_T$	109
Revolution Period, $T_0$	0.291 ms
Init. Normal. rms Emittance	$1 \pi$ mm mrad
coil inner radius / rms beam size	60
rf Frequency	360 MHz
Harmonic Number, h	17,450
Bunch Separation	5 m
Missing Bunches	4 out of 5
q	0.5
f	1.118
$\beta^*$	0.5 m

The results are shown in Table 3 and in the Figures 1 to 12. We discuss below the results.

Table 3: Fixed-Size Approach with variable Energy

Kinetic Energy, TeV	20	40	60	80	100
Magnetic Rigidity, Tm	66716	133429	200142	266855	333567
Bending Field, Tesla	6.55	13.10	19.65	26.20	32.75
Quad Gradient, Tm/cm	10.48	20.97	31.45	41.93	52.42
Energy Loss/Turn, MeV	0.122	1.955	9.899	31.286	76.382
E-Damping Time, min	793	99	29.4	12.4	6.35
Energy Spread @ equil	$2.16 \times 10^{-6}$	$4.32 \times 10^{-6}$	$6.47 \times 10^{-6}$	$8.63 \times 10^{-6}$	$10.8 \times 10^{-6}$
rms Emittance, mm mrad	$0.36 \times 10^{-7}$	$1.46 \times 10^{-7}$	$3.27 \times 10^{-7}$	$5.82 \times 10^{-7}$	$9.09 \times 10^{-7}$
Injection Energy, TeV	2	4	6	8	10
Emittance @ Injection	$4.69 \times 10^{-4}$	$2.35 \times 10^{-4}$	$1.56 \times 10^{-4}$	$1.17 \times 10^{-4}$	$0.94 \times 10^{-4}$
Emittance Reduction	1290	161.2	47.8	20.2	10.3
Magnet Bore diam., mm	45.6	32.2	26.3	22.8	20.4
Luminosity, $\text{cm}^{-2} \text{s}^{-1}$	$1.0 \times 10^{33}$	$4.0 \times 10^{33}$	$9.0 \times 10^{33}$	$16.0 \times 10^{33}$	$25.0 \times 10^{33}$
Protons / Bunch	$7.41 \times 10^9$	$0.83 \times 10^9$	$1.86 \times 10^9$	$3.30 \times 10^9$	$5.16 \times 10^9$
Beam Current, mA	71	7.9	17.9	31.7	49.6
Radiated Power, W/m	0.100	0.178	2.027	11.39	43.45
rf Peak Voltage, MV	20	40	60	80	100
rf Phase Angle, degrees	0.350	2.802	9.496	23.021	49.802
Phase-Oscill. Freq., Hz	4.071	4.069	4.043	3.905	3.271
rms Bunch Length, cm	6.00	0.426	0.643	0.887	1.324
$\sigma^*$ , $\mu\text{m}$	4.84	0.270	0.405	0.539	0.674
Crossing Angle, $\mu\text{rad}$	80.8	63.4	63.0	60.8	50.9
Beam-Beam Tune-Shift	0.00085	0.0153	0.0102	0.00767	0.00614
Peak Current, A	2.37	3.72	5.54	7.13	7.47
Z/n, ohm	5.33	0.051	0.115	0.211	0.393

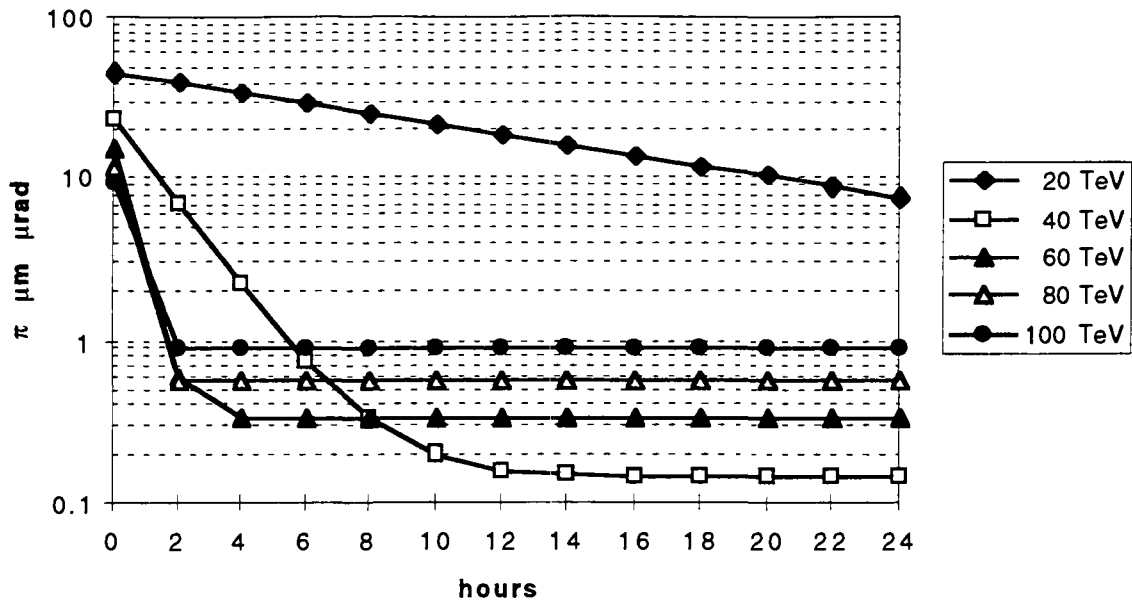


Figure 1. This is the display of the rms emittance with time during a storage period of 24 hours. It is seen that the effects of the synchrotron radiation are marginal at 20 TeV, but that they are already very significant at 40 TeV, when the final equilibrium dimensions are reached half-way the storage period. Thus, in the following, the effects of the synchrotron radiation are neglected at 20 TeV. For energies values larger or equal to 40 TeV, the collider performance is estimated assuming that the equilibrium dimensions have been reached. Actually, the integrated luminosity is 50% of the final value at 40 TeV, and about or better than 90% for large energies.

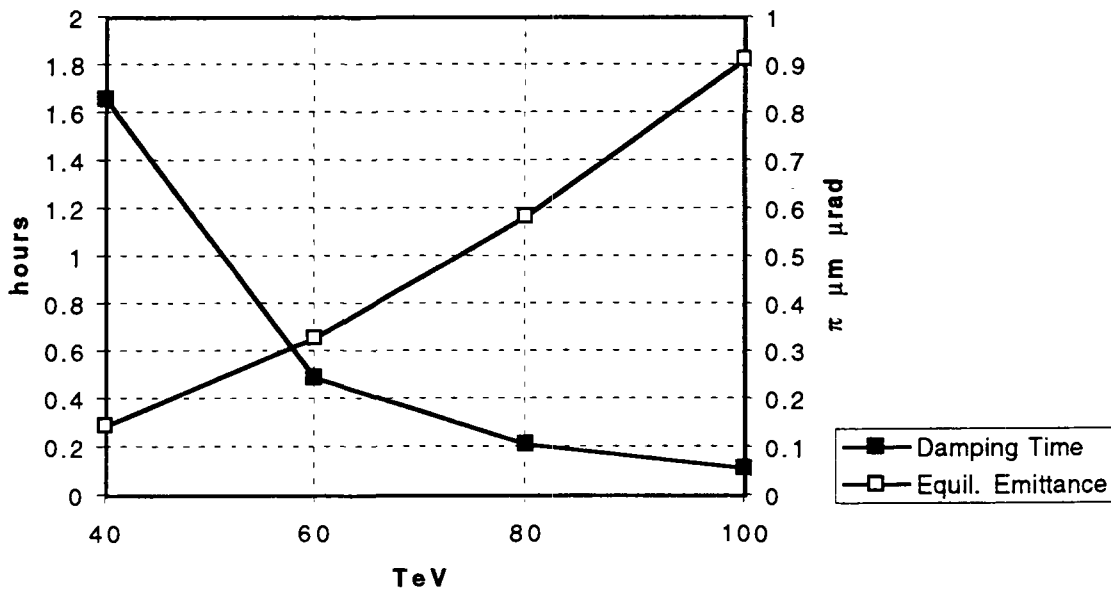


Figure 2. This shows the synchrotron radiation damping time and the equilibrium emittance with beam energy. At 100 TeV, the damping time is about 10 minutes, but the equilibrium emittance is close to  $10^{-6} \pi \text{ mm mrad}$ .

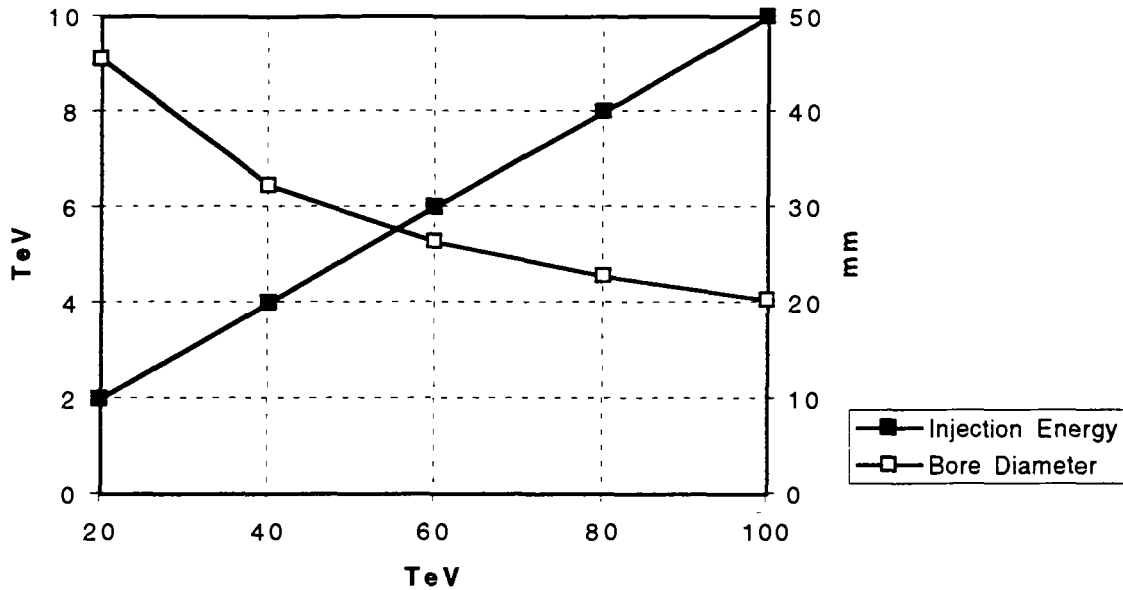


Figure 3. We assume a factor of 10 in energy between injection and storage, as it was also in the SSC design. The narrow energy excursion is required to eliminate adverse effects caused by the saturation and persistent currents in the superconducting magnets. The required magnet coil internal diameter is also shown in the figure. Scaling from the estimates for the SSC, a coil i.d. of 20 mm will suffice at the energy of 100 TeV.

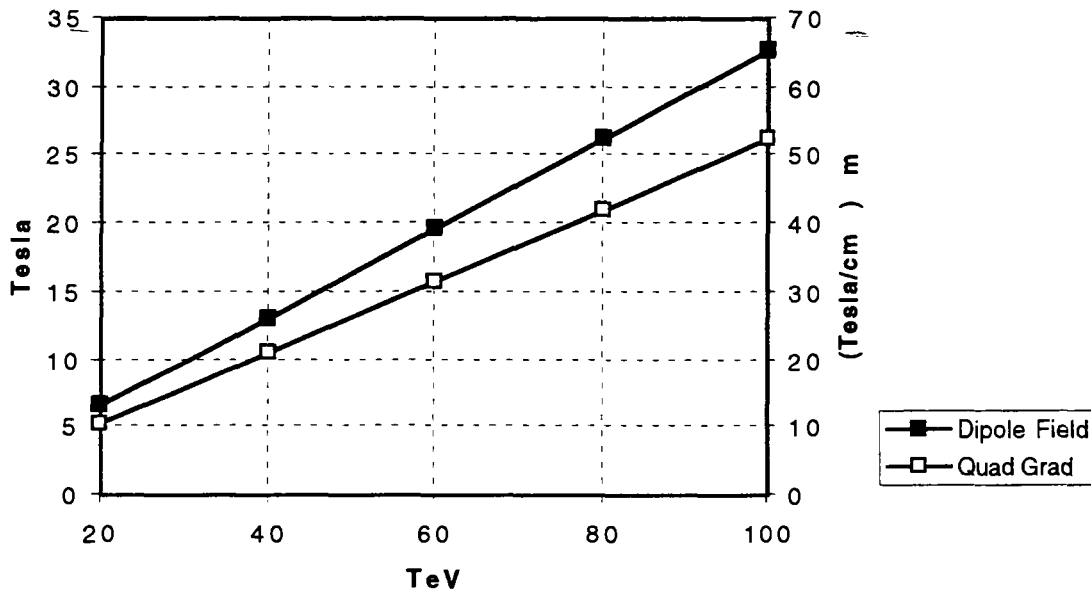


Figure 4. The required bending field and the integrated gradient of the quadrupoles are shown versus the beam energy. The value at 20 TeV equals that of the SSC design. At 40 TeV, the field is 13 Tesla, obviously twice that of the SSC, which may be within reach in a near future with extrapolation of the present technology. Beyond this, there are large unknowns, and very likely a 100 TeV beam cannot circulate in such a small collider size.

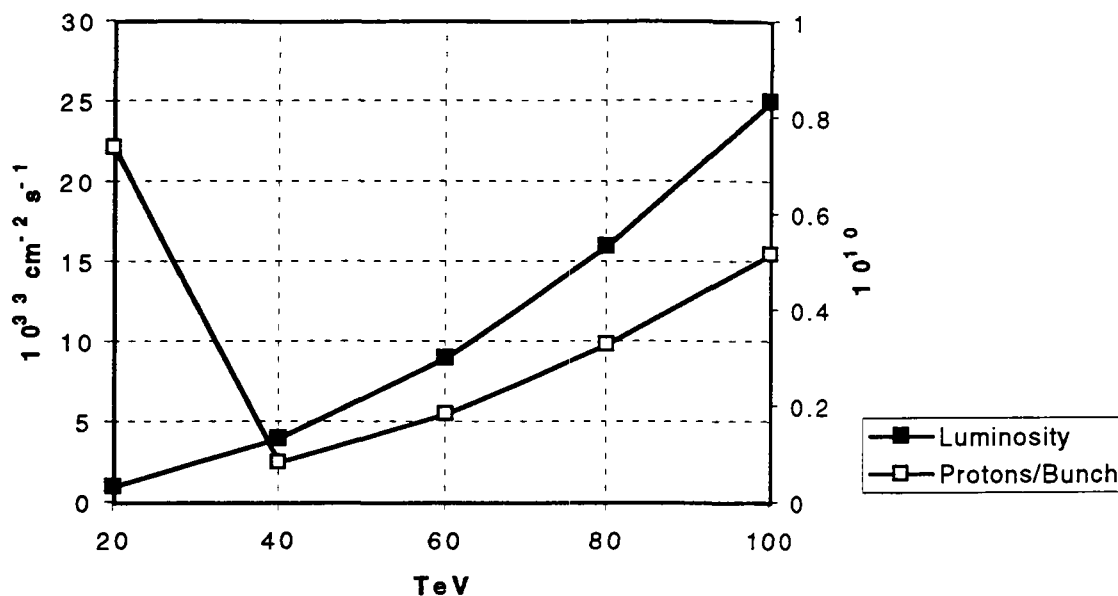


Figure 5. We have assumed a luminosity that increases quadratically with the beam energy and has a value of  $1 \times 10^{33} \text{ cm}^{-2} \text{ s}^{-1}$  at 20 TeV as it was originally required in the SSC design. Since we know the number of beam bunches, the revolution frequency and the equilibrium beam emittance, we can calculate how many protons per bunch are required for  $\beta^* = 0.5 \text{ m}$ . The discontinuity at 40 TeV is caused by the assumption that the emittance at 20 TeV is determined by the injector. It is seen that the total number of protons required is always less than that required at 20 TeV.

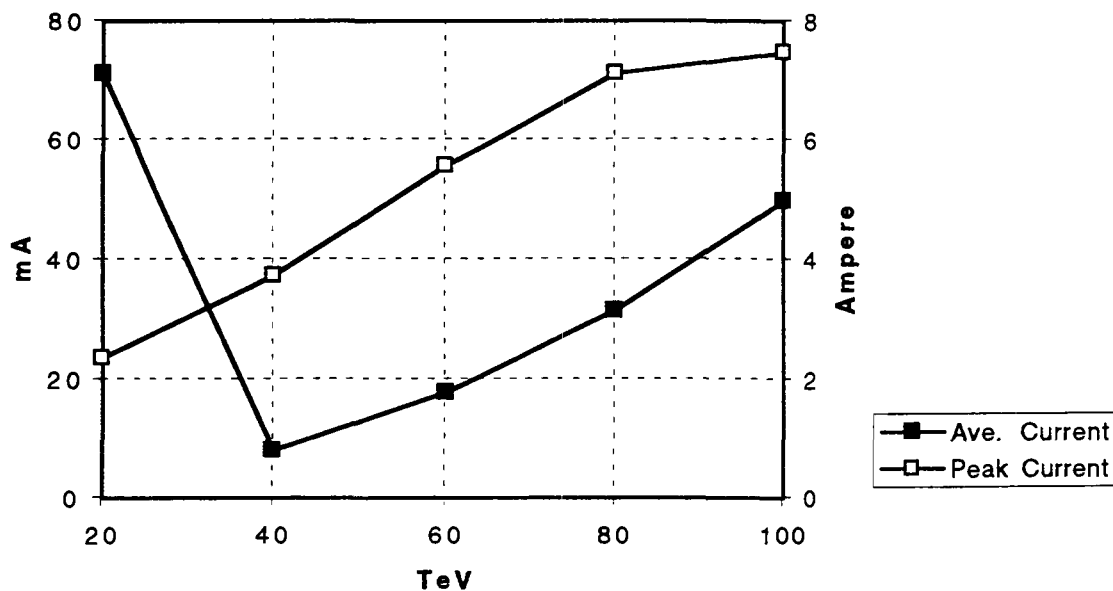


Figure 6. The discontinuity at 40 TeV in this and other Figures has already been explained. The bunch peak current increases with the beam energy. It depends on the bunch length which is shown in Figure 9.

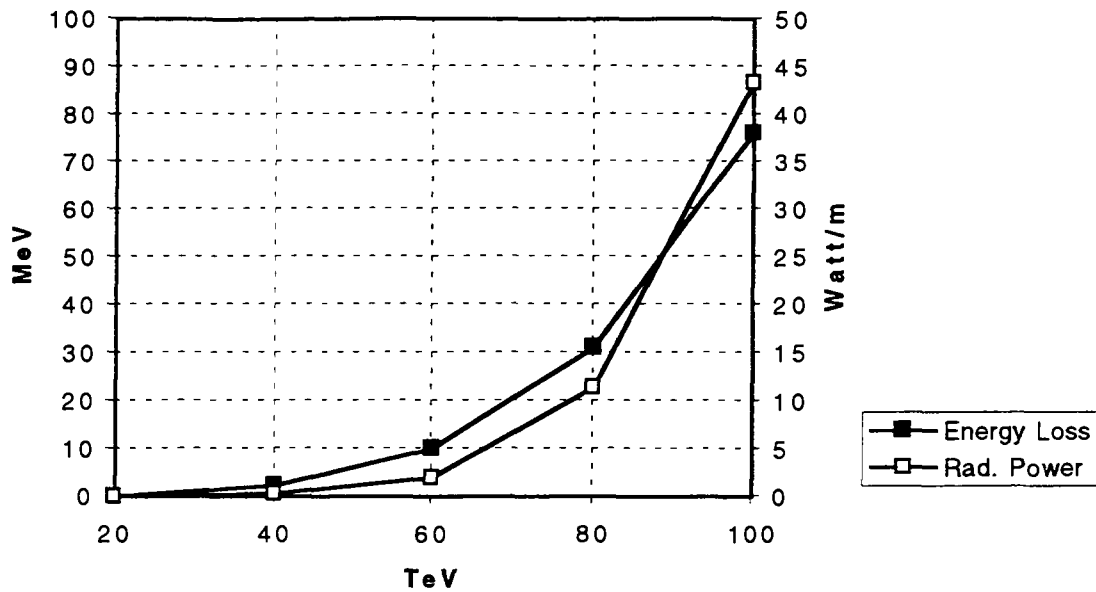


Figure 7. The energy loss per revolution per proton increases with the fourth power of the beam energy. Also the power radiated per unit length by the total beam increases correspondingly. At 100 TeV the energy loss is about 80 MeV per turn and the power radiated by the beam is 44 W/m. These are large values. The energy loss can eventually be compensated by the accelerating rf system. On the other end, the radiated power causes some serious consequences on the design of the vacuum and cryogenic systems.

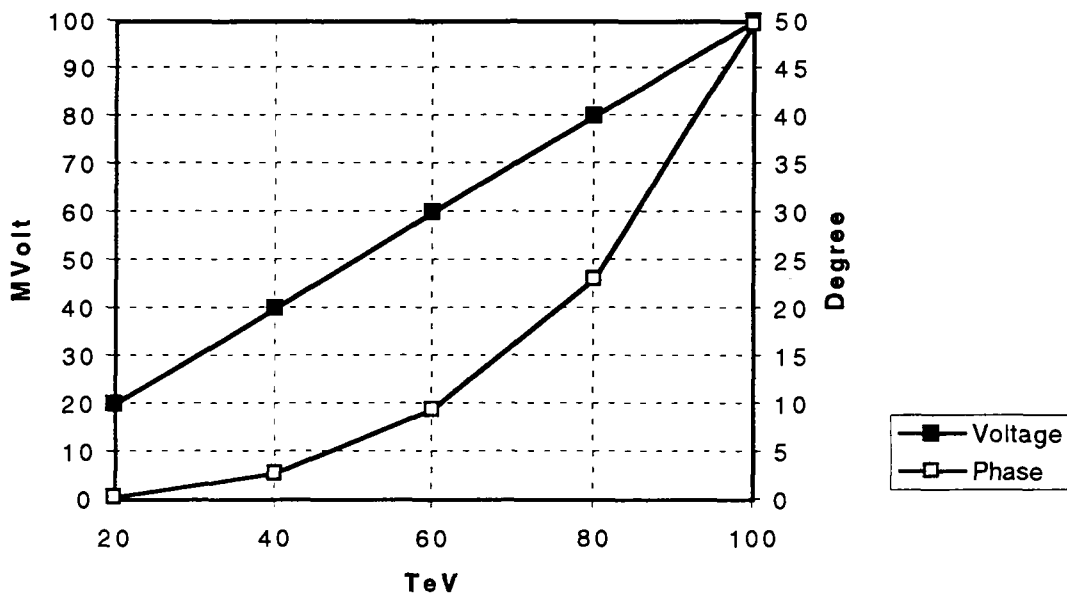


Figure 8. We have assumed a linear variation of the peak rf voltage with beam energy. Consequently, the rf phase angle has also to be adjusted to provide compensation for the energy loss, and the rf buckets are to be large enough to surround adequately the proton bunches.



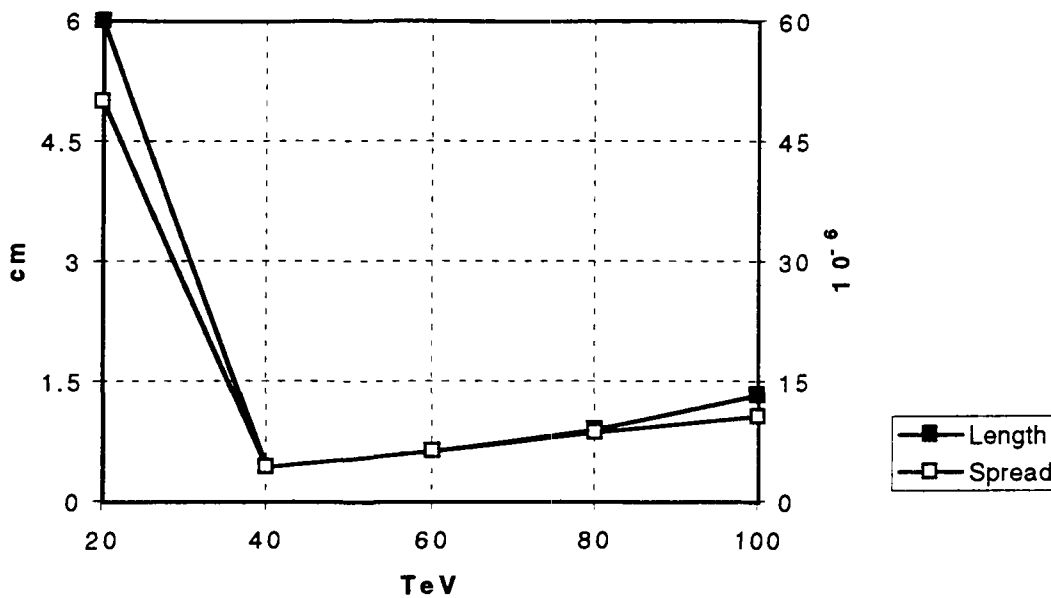


Figure 9. The effects of the synchrotron radiation are obviously very pronounced at large energies. The equilibrium energy spread, and, thus, the equilibrium bunch length are rather small. There is some concern on the individual bunch stability against coherent oscillations which we shall address later on.

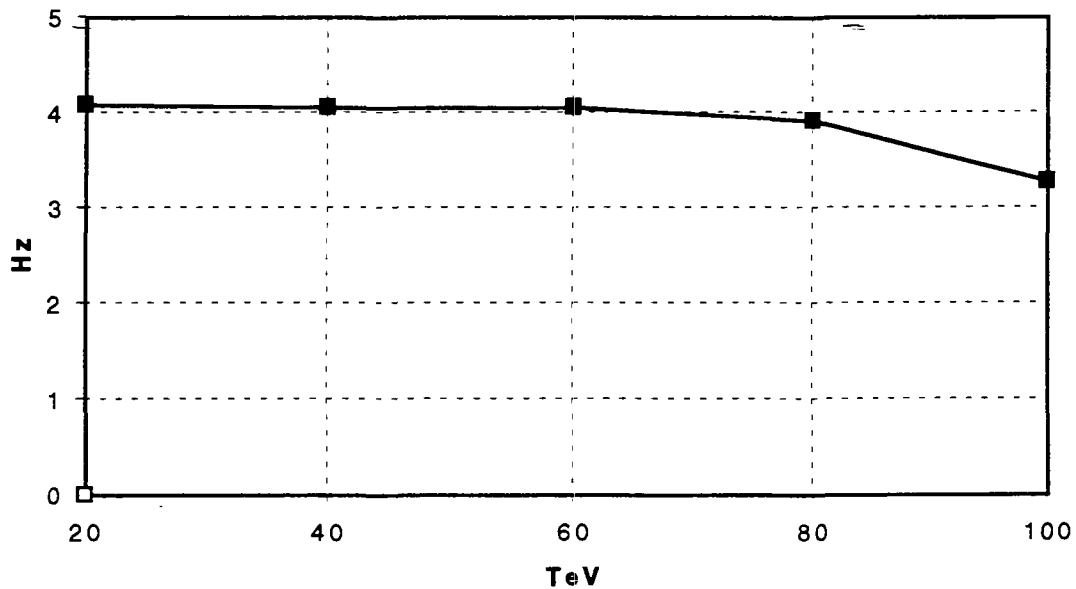


Figure 10. This shows the phase oscillation frequency versus beam energy. It varies between 3 and 4 Hz, which are rather low values. There is then the concern about noise entering the rf system at these frequencies.

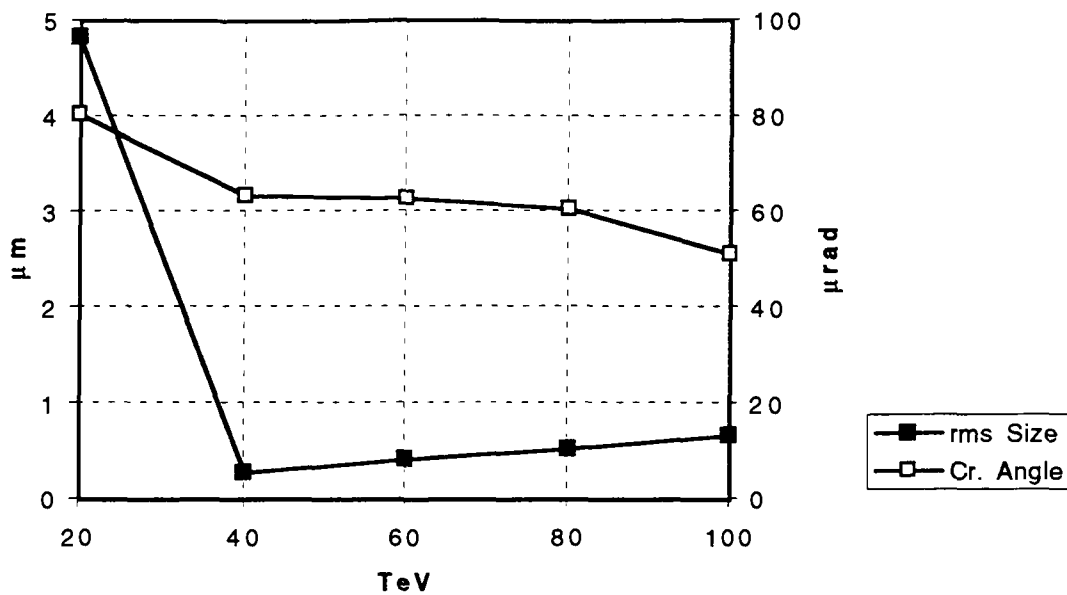


Figure 11. Since the form factor  $q$  has been assigned, we can determine the required crossing angle from the rms bunch length and the rms beam spot size at the collision point. The total crossing angle is around  $60 \mu\text{rad}$ .

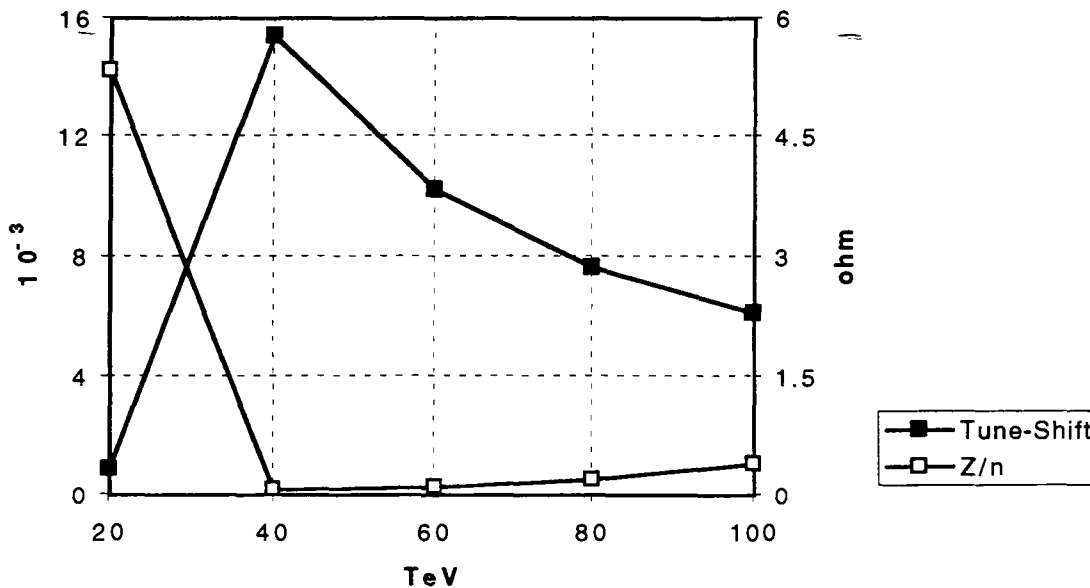


Figure 12. Finally, the beam-beam tune-shift and the longitudinal coupling impedance limit  $Z/n$  are plotted in this Figure versus the beam energy. The tune shift is large, but it decreases with the beam energy. At 100 TeV one has  $\Delta\nu = 0.006$ . Is this acceptable? In the SSC design  $\Delta\nu = 0.0005$ . Also the  $Z/n$  limit is rather small, only 0.3 ohm at 100 TeV, whereas at 20 TeV (SSC) it was 5 ohm.

In conclusion, a hadron collider designed with the fixed-size approach, with a circumference of 87.2 km, in principle could operate up to an energy of 40 TeV, provided that a 13-Tesla magnet could be developed. The major points of difficulty and concern are as follows:

(i) Clearly the small size, equivalent to the one proposed for the SSC, does not make operation possible at 100 TeV. A superconducting magnet with a very large field needs to be developed. It seems that the present technology will not be capable to do this. If 100 TeV is desired, then a larger collider circumference is needed.

(ii) Synchrotron radiation effects are important and useful only for energies larger than 40 TeV. These effects enhance the collider performance up to an energy of about 300 TeV. For large energy values, the benefits from the synchrotron radiation effects are lost.

(iii) The injector to the collider is not a trivial accelerator complex. For a final beam energy of 100 TeV, an injection energy of 5 to 10 TeV is required, which is comparable to the Large Hadron Collider.

(iv) The requirement for the magnet aperture is reduced at large energies. It is possible to take advantage of this up to a limit. A coil i.d. of less than 20 mm is likely not technically feasible.

(v) The beam intensity requirement is modest at large energies up to about 120 TeV. This simplifies the design and operation of the injector complex.

(vi) The radiated power is excessive at large energies. It represents quite a load to the refrigeration system, and pose a significant burden on the vacuum system due to the wall desorption effects.

(vii) The individual bunch stability as expressed by the threshold value of the longitudinal coupling impedance  $Z/n$  may be a point of concern and an issue to be re-investigated.

(viii) The large beam-beam tune-shift is also a major concern for the long-term beam stability.

### **Fixed-Field Approach**

In this approach we shall keep the same value of the bending field to 13 Tesla, twice the value originally adopted for the SSC project. As we vary the beam energy between 20 and 100 TeV, the circumference of the collider will be calculated accordingly. Again, we shall make use of some parameters which are common to all energies and that are closely derived from the SSC design. The parameters common to all energies are listed in Table 4. We shall assume the same packing factor, and thus a variable bending radius. All other parameters are similar to those also used in the fixed-size approach. In particular it results that the magnet Bore Diameter is the same at all energies, and of about 32 mm. Also the number of expected events per crossing does not change with beam energy and it is rather large.

The results are shown in Table 5 and displayed in Figures 13 to 24. They are discussed below.

Table 4: Parameters of the Fixed-Field Approach

Bending Field	13 Tesla
Quadrupole Gradient	21 (T/cm) m
Packing Factor	0.734
Number of FODO Cells	488
Phase Advance / Cell	90°
Betatron Tunes (H = V)	122
Bending Angle / Cell	12.87 mrad
$\gamma_T$	110
Initial Normalized rms Emittance	1 $\pi$ mm mrad
Bore Radius to rms Beam Size	60
Magnet Bore Diameter	32 mm
rf Frequency	360 MHz
Missing Bunches	5
Bunch-to-Bunch Separation	5.00 m
p	0.5
f	1.118
$\beta^*$	0.5 m
Number Events / Crossing	20

Table 5: Fixed-Field Approach with variable Energy

Kinetic Energy, TeV	20	40	60	80	100
Circumference, km	43.931	87.860	131.789	175.718	219.646
Revolution Period, $\mu$ s	146.5	293.1	439.6	586.1	732.7
FODO Cell Length, m	90	180	270	360	450
$\beta$ - max, m	153.6	307.3	460.9	614.6	768.2
$\eta$ - max, m	0.78	1.57	2.35	3.14	3.92
Energy Loss/Turn, MeV	0.243	1.940	6.549	15.524	30.321
E-Damping Time, min	201	101	67.1	50.3	40.3
Energy Spread @ equil	$3.04 \times 10^{-6}$	$4.30 \times 10^{-6}$	$5.26 \times 10^{-6}$	$6.08 \times 10^{-6}$	$6.80 \times 10^{-6}$
rms Emittance, mm mrad	$0.36 \times 10^{-7}$	$1.42 \times 10^{-7}$	$3.20 \times 10^{-7}$	$5.69 \times 10^{-7}$	$8.89 \times 10^{-7}$
Injection Energy, TeV	2	4	6	8	10
Emittance @ Injection	$4.69 \times 10^{-4}$	$2.35 \times 10^{-4}$	$1.56 \times 10^{-4}$	$1.17 \times 10^{-4}$	$0.94 \times 10^{-4}$
Emittance Reduction	1319	164.9	48.9	20.6	10.6
Harmonic Number	52,754	105,505	158,256	211,007	263,758
Number of Bunches	8,792	17,584	26,376	35,168	43,960
Protons / Bunch	$7.41 \times 10^9$	$0.82 \times 10^9$	$1.84 \times 10^9$	$3.26 \times 10^9$	$5.10 \times 10^9$
Beam Current, mA	71	7.8	17.7	31.4	49.0
Radiated Power, W/m	0.393	0.173	0.877	2.77	6.77
rf Peak Voltage, MV	20	40	60	80	100
rf Phase Angle, degrees	0.695	2.781	6.267	11.189	17.650
Phase-Oscill. Freq., Hz	5.691	4.022	3.276	2.819	2.485
rms Bunch Length, cm	6.00	0.422	0.635	0.853	1.081
$\sigma^*$ , $\mu$ m	4.84	0.267	0.400	0.533	0.667
Crossing Angle, $\mu$ rad	80.8	63.1	63.0	62.5	61.6
Beam-Beam Tune-Shift	0.00085	0.0155	0.0103	0.00776	0.00621
Peak Current, A	2.37	3.70	5.54	7.33	9.04
Z/n, ohm	5.25	0.050	0.075	0.100	0.127

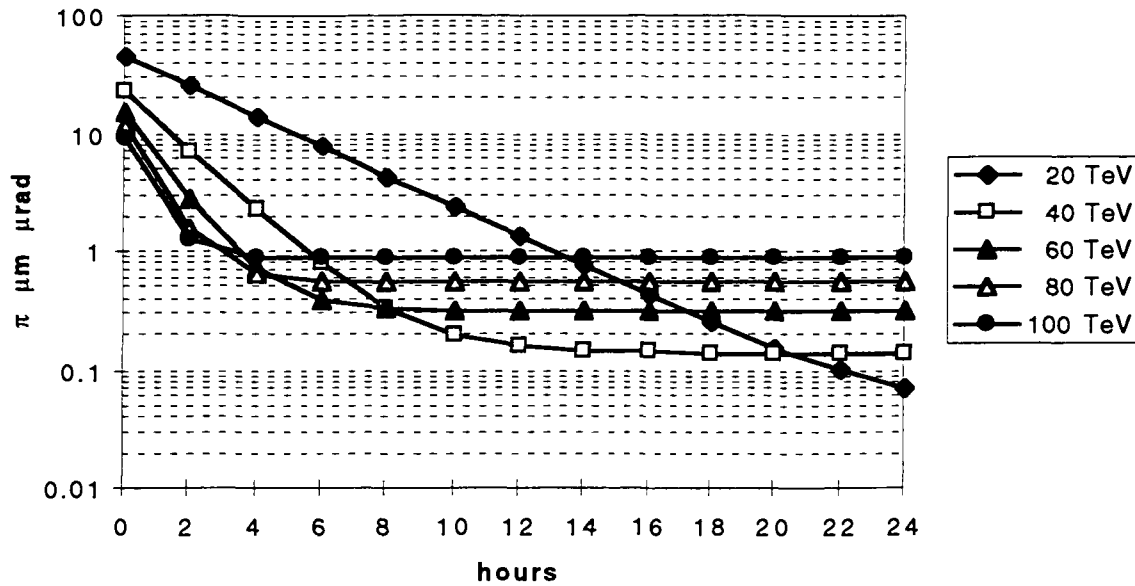


Figure 13. rms Betatron Emittance for different values of Beam Energy during a Colliding-Beam Cycle with a period of 24 hours. With the exception of the 20 TeV case, the results look similar to those found for the Fixed-Size Approach. In particular, the final luminosity is also about the same. Since the Damping Time is nevertheless longer, as shown below, the Average Luminosity is somewhat lower.

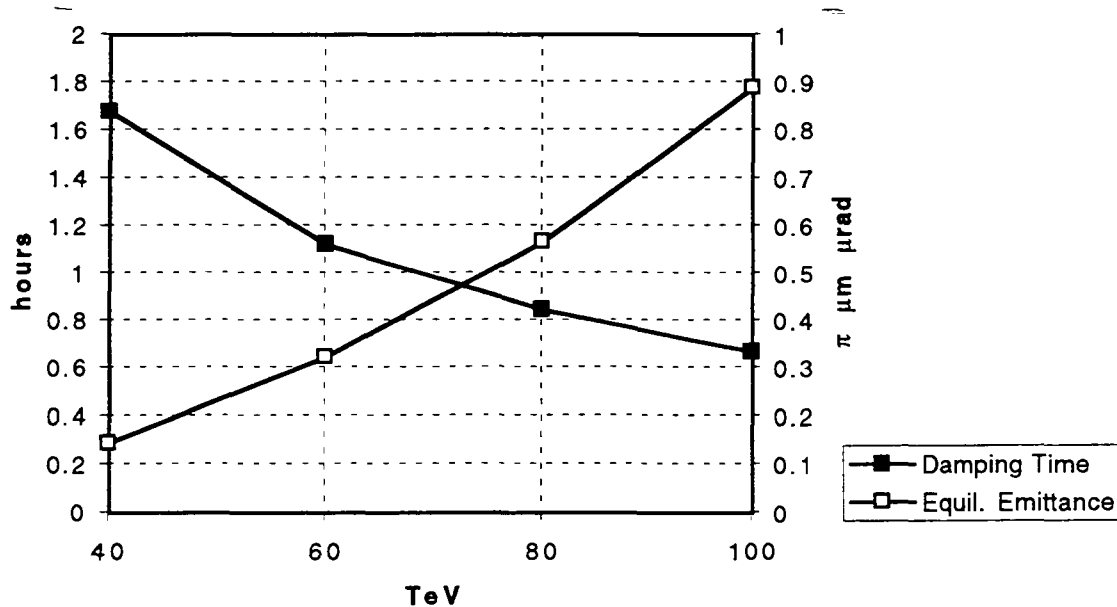


Figure 14. Equilibrium rms Emittance and Energy Damping Time versus the Beam Energy for the Fixed-Field (13 Tesla) Approach. The Equilibrium Emittance is just about the same as in the case of the Fixed-Size Approach. But the Damping Time is now considerably longer.

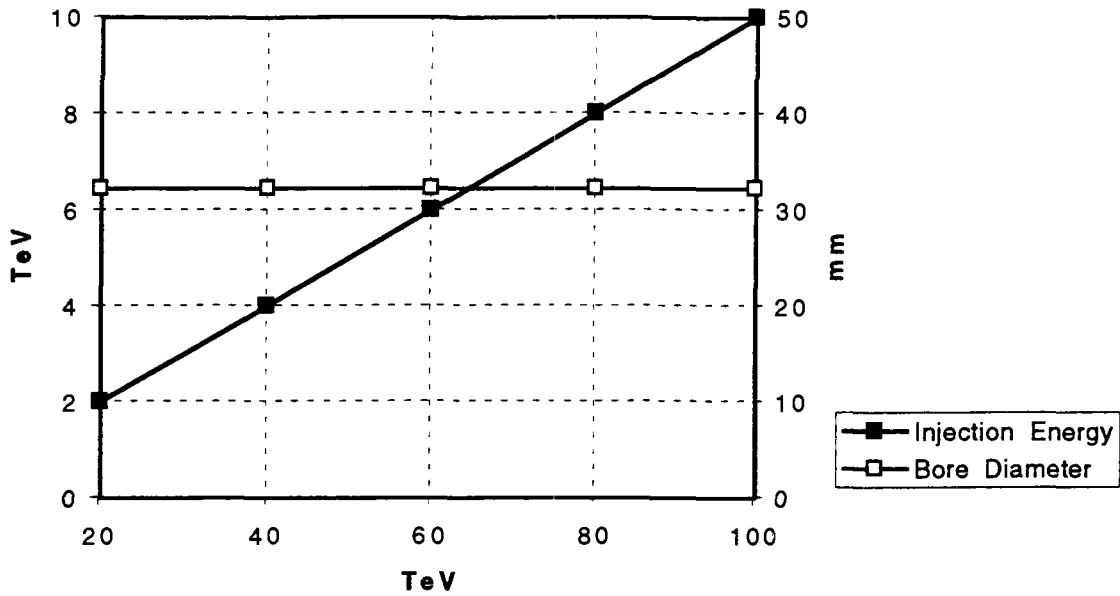


Figure 15. Injection Energy and Magnet Bore Diameter versus the Beam Energy for the Fixed-Field (13 Tesla) Approach. The Magnet Bore Diameter is now independent of the Beam Energy.

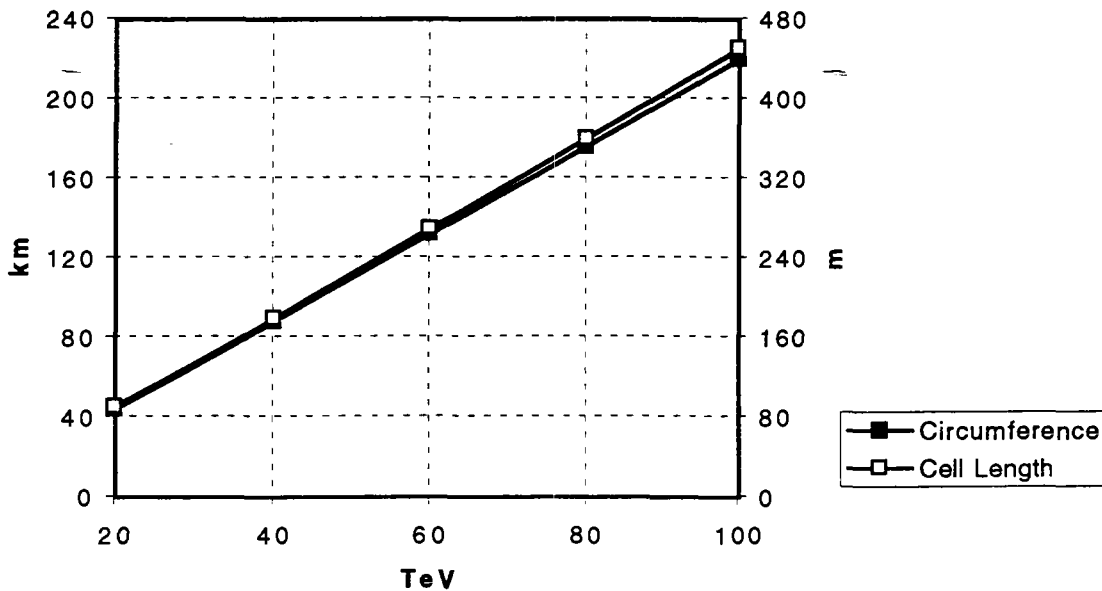


Figure 16. Collider Circumference and Length of FODO Cells versus the Beam Energy for the Fixed-Field Approach (13 Tesla). Both quantities increase linearly with Beam Energy. The gradient of the regular Quadrupoles and the Phase Advance per Cell have been assumed constant. Thus the Number of Betatron Oscillations per revolution is also independent of Beam Energy. At 100 TeV one needs a circumference of about 220 km.

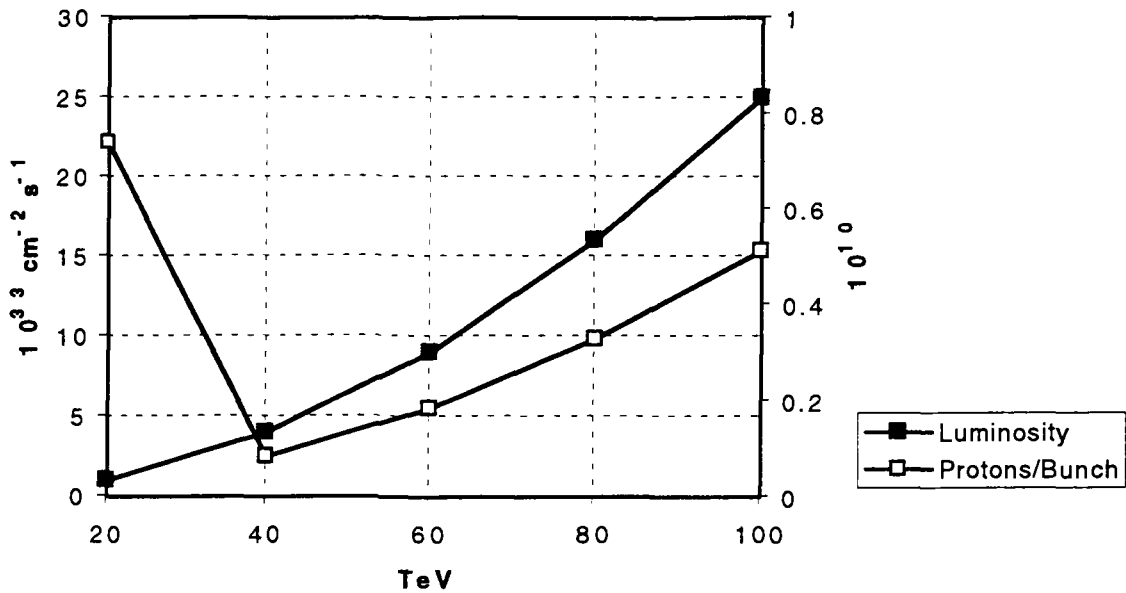


Figure 17. Luminosity and Number of Protons per Bunch versus the Beam Energy for the Fixed-Field (13 Tesla) Approach. The scaling assumption of the Luminosity with the Beam Energy is the same in both Approaches. It derives that the Number of proton per Bunches is also unchanged. As a consequence, because of the variation of the Collider Circumference with the Beam Energy, the total Number of Protons and of Bunches increases with the Beam Energy, as it is shown later.

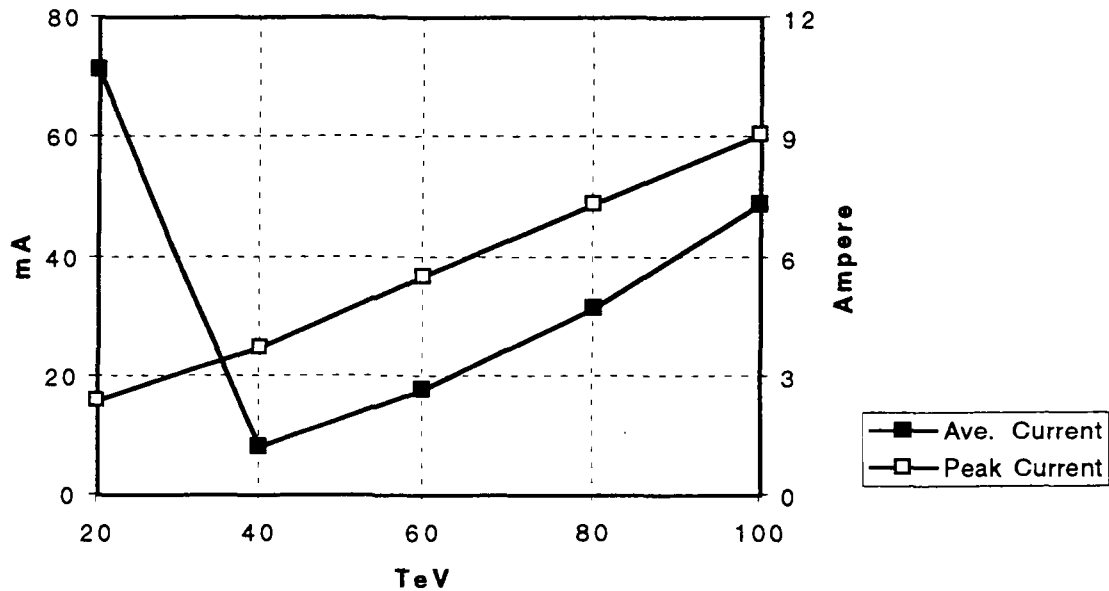


Figure 18. Average and Peak Beam Current versus the Beam Energy for the Fixed-Field (13 Tesla) Approach. The results are very similar to those found for the Fixed-Size Approach. The same considerations apply.



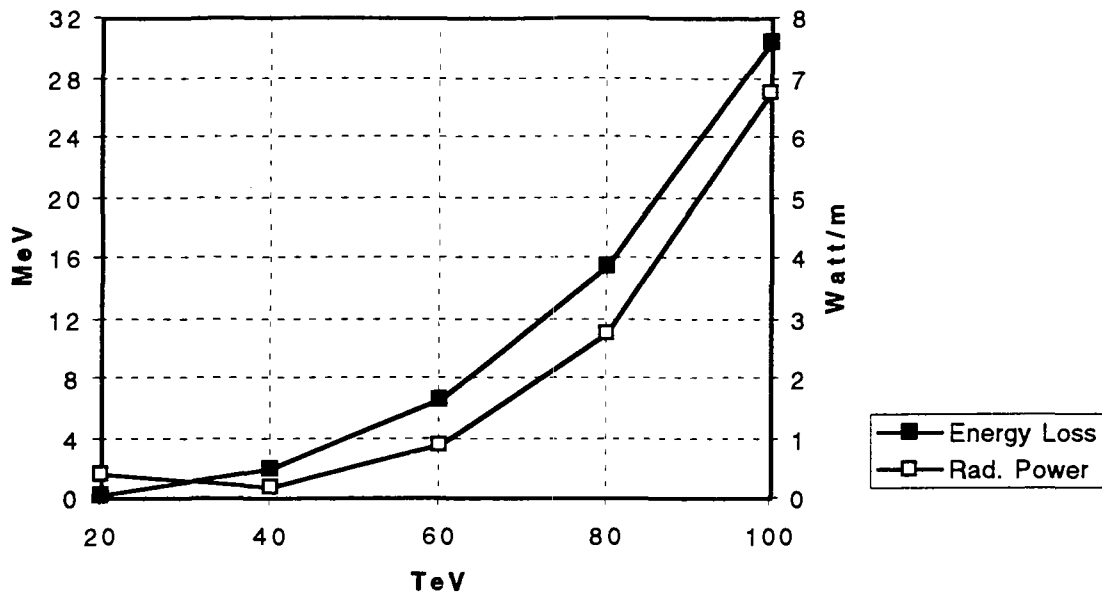


Figure 19. Energy Loss and Radiated Power per Unit Length versus Beam Energy for the Fixed-Field (13 Tesla) Approach. The Radiated Power is considerably smaller for the higher energies compared to the Fixed-Size Approach, because of the larger circumference of the Collider.

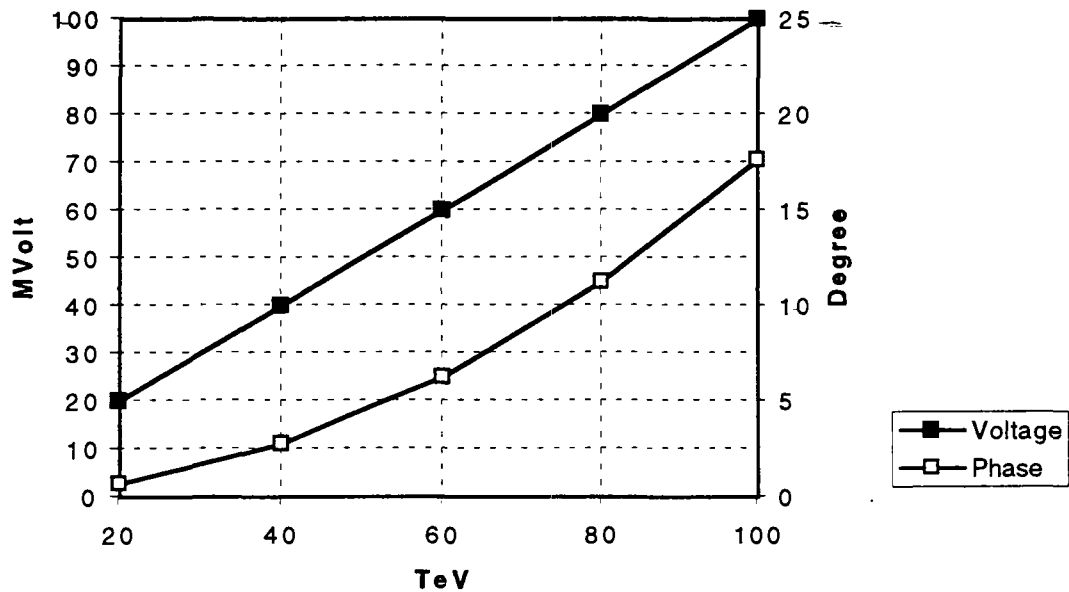


Figure 20. rf Peak Voltage and Phase versus Beam Energy for the Fixed-Field (13 Tesla) Approach. We have adopted a rf program similar to the one for the Fixed-Size Approach. The rf Phase is now somewhat lower. Otherwise the results are similar, and the same considerations apply.

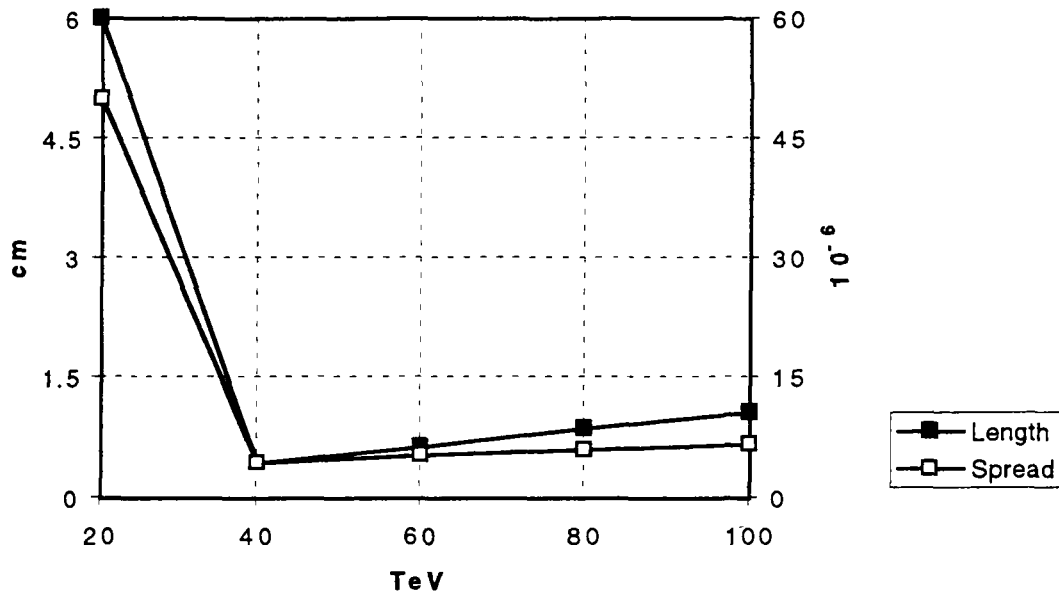


Figure 21. rms Bunch Length and rms Energy Spread versus Beam Energy for the case of Fixed-Field (13 Tesla) Approach. The results are similar to those found for the case of Fixed-Size Approach. Same considerations apply.

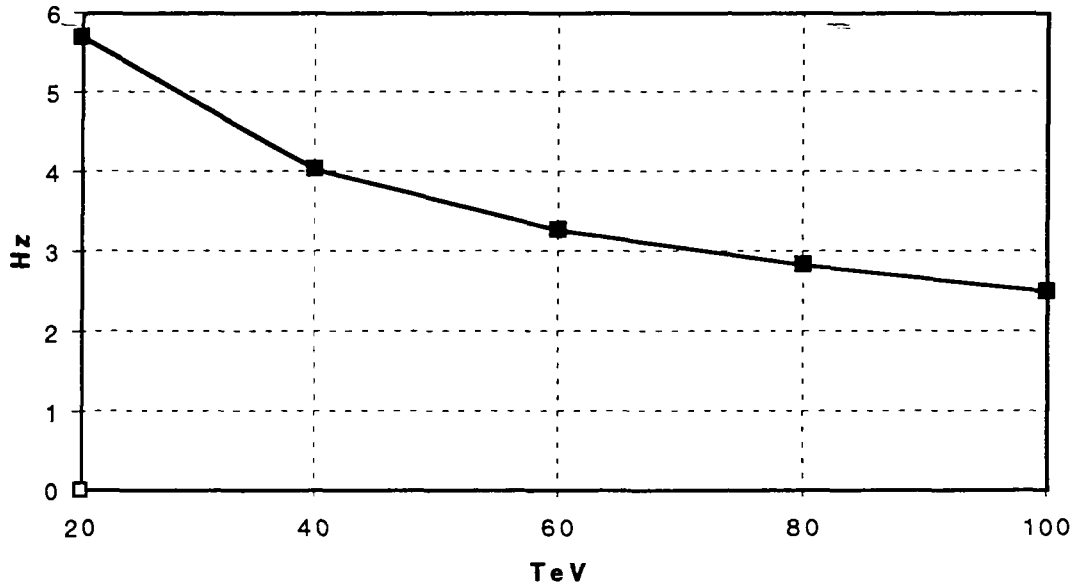


Figure 22. Phase-Oscillation Frequency versus Beam Energy for the Fixed-Field (13 Tesla) Approach. The results are similar to those found for the Fixed-Size Approach, mostly because we have also assumed similar rf System. The same considerations, of course, apply.

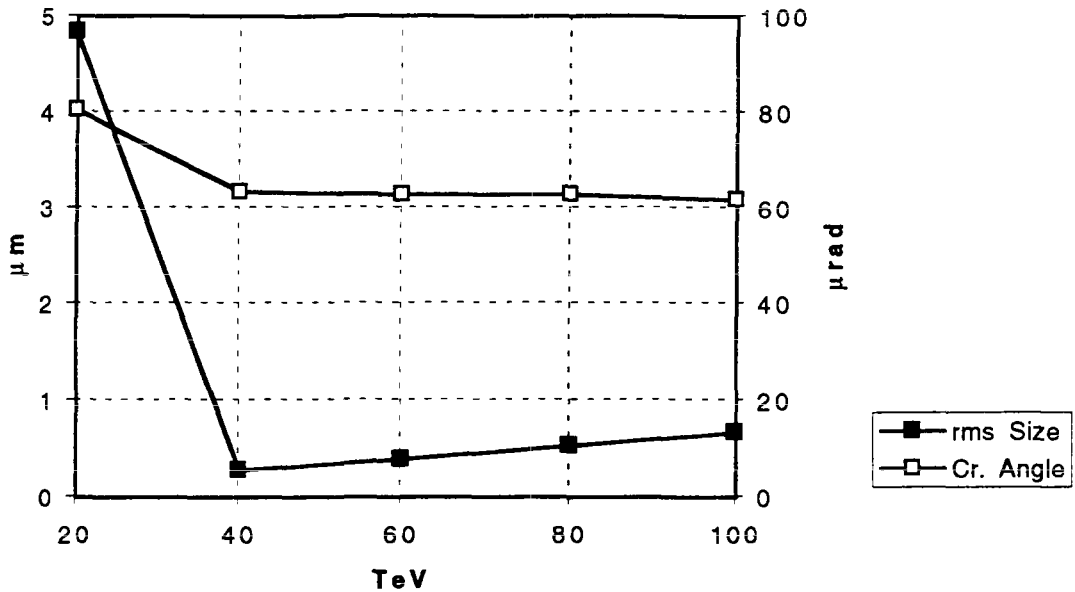


Figure 23. rms Beam Size at the Interaction Point and Crossing Angle versus the Beam Energy for the Fixed-Field (13 Tesla) Approach. The results are similar to those found with the Fixed-Size Approach. The same considerations apply.

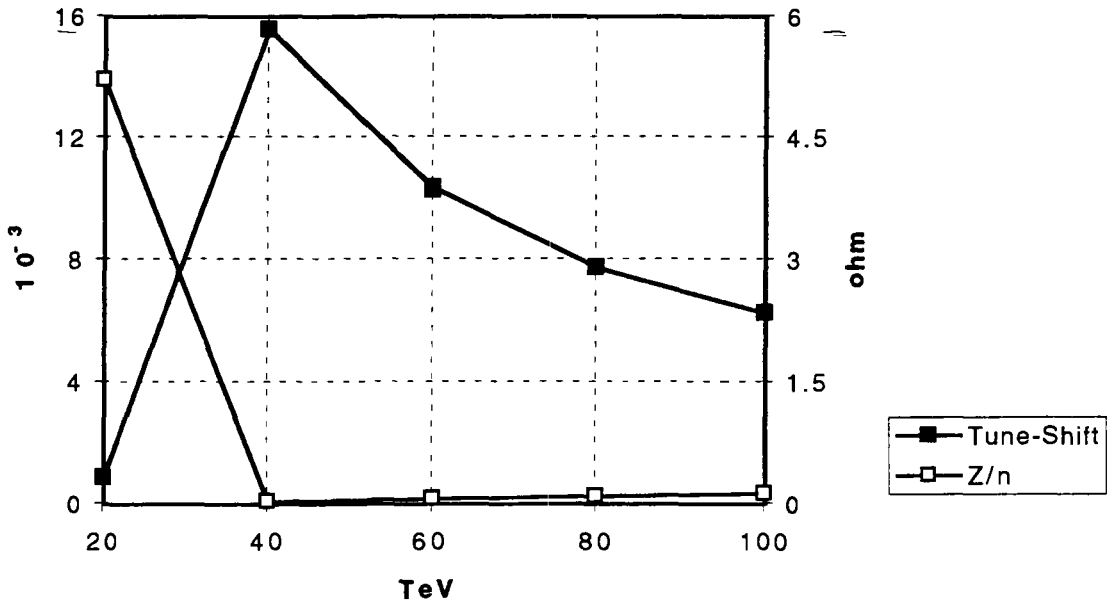


Figure 24. Beam-Beam Tune-Shift and Z/n Longitudinal Coupling Impedance Limit versus the Beam Energy for the Fixed-Field Approach (13 Tesla). One has results similar to those found with the Fixed-Size Approach. The same considerations apply.

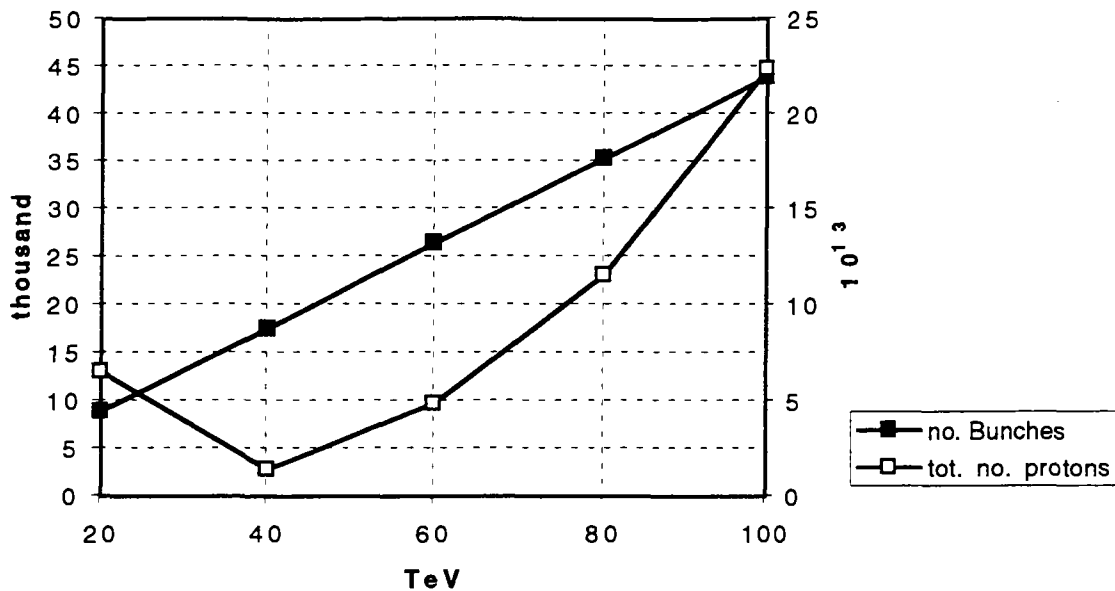


Figure 25. Total Number of Bunches and Total Number of Protons versus Beam Energy. The Total Number of Bunches increases linearly with the Beam Energy. The Total Number of Protons has a minimum in correspondence of 40 TeV.

## Conclusions

Remarkably the two approaches of Fixed-Size and Fixed-Value for estimating the Collider performance, dominated by synchrotron radiation effects, have given about the same result. Still a collider with the largest feasible bending field is desirable because enhances the effects of the synchrotron radiation on the performance. Already a field of 13 Tesla is adequate for the purpose. The SSC value of 6.5 Tesla on the other end is marginal, though the higher the beam energy the more effective are the synchrotron radiation effects.

There are nonetheless some concerns about the very small beam bunch dimensions, both longitudinal as well transverse, caused by the synchrotron radiation. Among some of them are: the beam-beam tune-shift, which at 100 TeV can be as large as 0.006; the  $Z/n$  limit of the longitudinal instability, which again at 100 TeV is low as 0.1 ohm; and, the coupled-bunch instabilities [3]. Also the loss of energy to synchrotron radiation are large. At 100 TeV with a bending field of 13 Tesla, the losses are 7 Watt per meter, which poses some serious uncertainties about the vacuum and cryogenic stability and cost.

## References

- [1] A. G. Ruggiero, Design Considerations and Expectations of a Very Large Hadron Collider. These Proceedings.
- [2] A. G. Ruggiero, Compendium of Equations for the Design of a Very Large Hadron Collider. These Proceedings.
- [3] F. Galluccio, M.R. Masullo, V.G. Vaccaro, Coherent Stability Criteria. These Proceedings